

Overland flow modelling with the Shallow Water Equation using a well balanced numerical scheme: Adding efficiency or just more complexity?

M. Rousseau^{*†}, O. Cerdan^{*}, O. Delestre^{‡§}, F. Dupros^{*},
F. James[§], S. Cordier[§]

January 30, 2012

Abstract

In the last decades, more or less complex physically-based hydrological models, have been developed that solve the shallow water equations or their approximations using various numerical methods. Model users may not necessarily know the different hypothesis lying behind these development and simplifications, and it might therefore be difficult to judge if a code is well adapted to their objectives and test case configurations. This paper aims at comparing the predictive abilities of different models and evaluating potential gain by using advanced numerical scheme for modelling runoff. We present four different codes, each one based on either shallow water or kinematic waves equations, and using either finite volume or finite difference method. We compare these four numerical codes on different test cases allowing to emphasize their main strengths and weaknesses. Results show that, for relatively simple configurations, kinematic waves equations solved with finite volume method represent an interesting option. Nevertheless, as it appears to be limited in case of discontinuous topography or strong spatial heterogeneities, for these cases we advise the use of shallow water equations solved with the finite volume method.

Keywords overland flow; well-balanced finite volume scheme; finite differences scheme; kinematic wave equations; shallow water equations; comparison of numerical models

1 Introduction

Shallow water runoff plays an essential role in natural ecosystems and is the main source of transfer of living and mineral elements in the landscape. In

^{*}Corresponding author: m.rousseau@brgm.fr, presently at: BRGM, 45060 Orléans Cedex 2, France

[†]Université Paris-Est, Cermics, Ecole des Ponts ParisTech, 77455 Marne la Vallée Cedex 2, France

[‡]Laboratoire de Mathématiques J.A. Dieudonné & EPU Nice–Sophia Antipolis, Université de Nice–Sophia Antipolis, Parc Valrose, 06108 Nice cedex 02, France

[§]MAPMO UMR CNRS 6628, Université d’Orléans, UFR Sciences, Bâtiment de mathématiques, B.P. 6759 – F-45067 Orléans cedex 2, France

areas modified by human activities (e.g. soil sealing), or during extreme climatic events, excess water runoff can lead to serious environmental issues such as the flooding of urban areas [7, 23], or the pollution of water bodies [6]. In order to prevent or to mitigate such events, it is therefore necessary to be able to predict the dynamic as well as the spatial extent of runoff production and transfer [59]. To meet this demand and to reflect the complexity of the processes involved as well as the spatial heterogeneity of the landscape, several modelling approaches of various complexities have been developed. Saint-Venant equations are adapted to describe shallow water flow [4]. They derive from the Navier-Stokes equations by averaging over depth, and assuming several hypothesis due to non linear terms [28, 62]. The Shallow Water equations (SW) can be simplified in various different forms [46] among which the simplest model is the Kinematic Wave model (KW) [56, 57], and another is the Diffusion Wave model (DW) [13]. These equations are highly nonlinear and therefore do not have global analytical solutions, so we have to approach the solution by numerical methods such as finite difference, finite element or finite volume.

The most commonly used is the Finite Difference method (FD) which is simpler over simple geometry (structured grid) and more intuitive. A key step is to replace the continuous derivatives with appropriate approximations in terms of the dependent variables evaluated at different mesh points in the region of interest. The basis for doing this is related to the Taylor Series expansion for a function in the vicinity of some discrete point, x_i . The Finite Element (FE) method is based on the variational formulation of the system. Usually, this method is not adapted to the discontinuous solutions, and not appropriated to solve conservative system of equations. The Finite Volume (FV) method is both adapted to any geometry (structured and unstructured meshes) and conservative by its formulation. It consists in solving the approached solution on each volume of the mesh (volumes in 3d, surfaces in 2d, and segments in 1d). Flux balance can be calculated (by integration of equations on these volumes) in each volume; the flux entering is then identical to that leaving the adjacent volume. This method is therefore conservative.

We can find many codes which solve SW or its approximations based on various numerical methods. For instance, to model hortonian overland flow on small plots [50] propose a model (PSEM_2D) based on a finite differences resolution with a Mac Cormack scheme coupling two-dimensional SW system with Green-Ampt infiltration model [30, 9]. They got a good agreement between the calculated results and the measured data on small plots in sandy soils. [38] used a two-dimensional KW model simulating runoff generation and flow concentration, based on two-dimensional KW theory and finite element method. Their comparisons with experimental observations, on an infiltrated hillslope receiving an artificial rainfall, were also satisfactory. [60] made comparisons on an experimental plot between simulated and observed flow-velocity field for three different models: PSEM_2D [50] a SW equations in 2D (presented previously), MAHLERAN [63] a 1D KW in the slope direction coupled with a 2D flow-routing algorithm, and Rillgrow2 [24] involving an empirical runoff algorithm (close to the DW equation in 2D). The results conclude that PSEM_2D was the most satisfying model, and MAHLERAN, though simple, obtained good results. [49] presented a two dimensional SW numerical model which uses the unstructured finite-volume method. The test case results, both analytical and experimental, validate the model and show that it is able to compute SW equations

on arbitrary and complex topographies. To model the storm runoff prediction from humid forested catchments, [36] developed a rainfall-runoff model for large scale, using a one dimensional KW approximation solved by an implicit finite difference scheme. Furthermore, to optimise the abilities of each model, it is possible to use both KW and DW. For instance, [47] proposed a distributed physiographic conceptual model using a finite difference method for, both KW and SW in function of the watershed decomposition in subwatersheds (according to the drainage area).

For these three methods (FD, EF, and FV), it is also necessary to chose a numerical scheme. It might be either implicit or explicit (in theory, implicit methods are unconditionally stable, but their use implies solving big systems). It might also be Forward, Backward, Centred or Upwind. Moreover, concerning FV, a numerical flux has to be chosen. There are several possible choices: Rusanov [8], VFRoencv [27], HLL [32],... The choice of this flux is based on several criterions: stability, water height positivity preserving, maximum principle preserving,... For example, [16] compares different fluxes for simulations of overland flow on agricultural surfaces, and concludes that it is preferable to chose HLL in this case. In addition, it is well-known that, since [5], the topography source term needs a special treatment which enables at least to preserve steady states at rest. The schemes having this property are said to be well-balanced [31]. In litterature, we may find a lot of such schemes (see among others see [3, 8, 35, 37, 51]).

Once chosen the resolution method and the numerical scheme, the source terms (other than the topography) might be treated under several ways: concerning the friction term, both a law (Manning, Chézy, linear,...) and the numerical treatment (explicit, implicit, semi-implicit) has to be chosen. Concerning infiltration, a coupling with another physical model is needed. Several choices of equations (Philip [52], Green-Ampt [30], Richards [53]) are possible [11]. There are different types of physical model coupling, for instance SW with Green-Ampt [22], or KW with Richards [58, 64]. This choice and the numerical method are governed by the process to simulate. Therefore it exists a vast number of possible resolutions, and an important number of hydrological models: by the choice of the equation system governing the processes to model, and by the used resolution method. For example, in the case of erosion process on catchments and for land management applications, KW with finite element method is predominantly used with erosion threshold laws [26] (EUROSEM [45], LISEM [15]).

Until now, KW and finite differences are the most used in hydrology, because of its simplicity and low computational costs (LISEM, KINEROS [65], WEPP [48]). However, SW is increasingly used in hydrological models such as [22, 25, 49] TELEMAC-2D, more complete equations allow to better model physical processes. In fact, everyone implements his own method, depending on its knowledge and means of computation; the model validation principally established on comparisons with observed data or analytical test cases [20, 19, 29]. Theses evaluations are generally only valid for a ponctual application and are thus not generic. Few comparisons of models based on their patterns have been done, therefore we can not know what advantages are obtained with the different methods in order to choose in function of the modelling aims [60].

In this context, this study aims at comparing the predictive abilities of different models and evaluating the interest to complicate a numerical scheme (to

take into account the different elements of the terrain and the geometry of the network flow) for modelling runoff. We will present four different codes with different governing equations and numerical resolution, and compare them on different test cases allowing to emphasize main strengths and weak points of the four options.

2 Methodology

2.1 Governing equations

2.1.1 Shallow Water equations

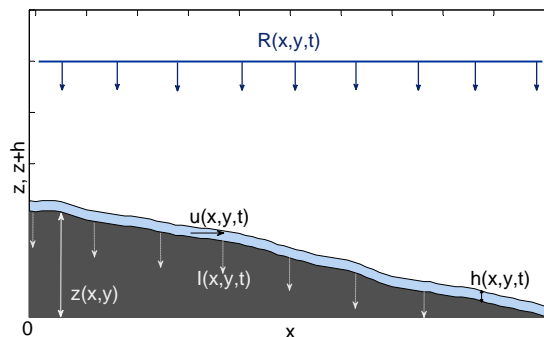


Figure 1: Geometric configuration and basic notations in x direction.

In this study, overland flow is described using the Shallow Water equations or Saint-Venant system [4] which are obtained from the 3D incompressible Navier-Stokes equations with some simplifying assumptions. The main operation giving Shallow Water equations from Navier-Stokes is an average over the vertical, however the existence of non linear terms requires some assumptions and approximations [34, 62].

First, we assume that the pressure is hydrostatic, *i.e.* the acceleration due to the pressure balances gravity, secondly we assume the water depth is much smaller than the characteristic horizontal size of the field of study. Next, we suppose that the vertical velocity is negligible and thus has no equation. Once these assumptions done, the Navier-Stokes equations (with mass constant volume and hydrostatic pressure) will be averaged on the vertical by integration from the bottom to the surface [28, 43].

In two space dimensions, the system of Shallow Water equations can be written as follow (see Figure 1):

$$\frac{\partial}{\partial t} h + \frac{\partial}{\partial x} hu + \frac{\partial}{\partial y} hv = S, \quad (1)$$

$$\frac{\partial}{\partial t} hu + \frac{\partial}{\partial x} (hu^2 + \frac{gh^2}{2}) + \frac{\partial}{\partial y} huv = -gh(S_{0_x} + S_{f_x}), \quad (2)$$

$$\frac{\partial}{\partial t} hv + \frac{\partial}{\partial x} huv + \frac{\partial}{\partial y} (hv^2 + \frac{gh^2}{2}) = -gh(S_{0_y} + S_{f_y}). \quad (3)$$

Where (1) is the equation of mass conservation, and (2)-(3) two momentum equations.

x and y [L] are the space coordinates, t [T] the time, h [L] the local vertical depth of water, u [L/T] and v [L/T] the depth-average velocities, S_0 [L/L] the bed slope and g [L/T²] the gravitational constant. The source term S [L/T] corresponds to the volume of water that is available, namely the difference between the rainfall rate R [L/T] and the infiltration rate I [L/T]; it can be expressed as follows: $S = R(x, y, t) - I(x, y, t)$

And, S_{f_x}, S_{f_y} [L/L] are energy grade line slope or friction terms. S_0 the bed slopes are calculated directly with ground surface elevation z [L]:

$$S_{0_x} = \frac{\partial z}{\partial x} \quad \text{and} \quad S_{0_y} = \frac{\partial z}{\partial y}. \quad (4)$$

2.1.2 Kinematic Waves

Many watershed codes are based on the kinematic wave theory for modelling hydrological processes in surface water. Kinematic Wave model is one of various simplifications existing of Shallow Water equation (seen previously), it is the simplest model and it combines the momentum and mass conservation equations [13]. It consists in neglecting the local acceleration, convective acceleration, and pressure terms in the momentum equation. That is to say, the main assumption is that the gravity and friction forces balance each other. So we have the continuity equation (1) and a motion equation that corresponds to the equality between component along the slope and the resistance force [38], equations (2)-(3) ($S_0 = S_f$). So the wave motion is principally described by the equation of continuity.

2.1.3 Friction term

In the equations (2)-(3), S_{f_x} and S_{f_y} are the friction terms. As regards its formulation, our study includes two options often used in hydrological studies: Manning's law (5) and Darcy-Weisbach's law (6) [22, 25, 40, 41]. Both of them are derived from empirical considerations [12, 62]:

$$S_{f_x} = K^2 \frac{u\sqrt{u^2 + v^2}}{h^{4/3}}, S_{f_y} = K^2 \frac{v\sqrt{u^2 + v^2}}{h^{4/3}}, \quad (5)$$

$$S_{f_x} = f \frac{u\sqrt{u^2 + v^2}}{8gh}, S_{f_y} = f \frac{v\sqrt{u^2 + v^2}}{8gh}. \quad (6)$$

Where K and f are respectively Manning's and Darcy-Weisbach's roughness coefficient which depend on physical and natural properties, estimated from calibration or published values (see for exemple tables in [12]). These coefficients are supposed to be constant in time during the example.

For the Kinematic Waves approximation, thanks to (2)-(3) we obtain the following expression for the velocity which depends on the choice of the friction's law:

$$\text{Manning:} \quad u = h^{8/3} \sqrt{|S_{0_x}|/K}, v = h^{8/3} \sqrt{|S_{0_y}|/K}, \quad (7)$$

$$\text{Darcy-Weisbach:} \quad u = h^{5/2} \sqrt{8g |S_{0_x}|/f}, v = h^{5/2} \sqrt{8g |S_{0_y}|/f}. \quad (8)$$

where $Q_a = h \cdot \Delta x$, with Δx the space step defined in Section 2.2. If the available water volume on a cell is smaller than the infiltration capacity: all is infiltrated, and otherwise infiltrated volume is equal to infiltration capacity and the remainder streams.

Values of these infiltration parameters for various soil classes can be found in [13, p.115]. Numerous studies show that the saturated hydraulic conductivity is the most influent one, [55] presents a study on the impact of this parameter on the surface runoff.

2.2 Numerical resolution

In this section, we present and describe four numerical discrete methods, in order to compare them subsequently. So we solve our system on a spatial discretization (see Figure 3), the domain is divided in cells (indexed by (i,j)) which writes $C_{i,j} = [x_{i,j} - \frac{\Delta x}{2}, x_{i,j} + \frac{\Delta x}{2}] \times [y_{i,j} - \frac{\Delta y}{2}, y_{i,j} + \frac{\Delta y}{2}]$ (respectively $C_{i,j} = [x_{i,j}, x_{i,j} + \Delta x] \times [y_{i,j}, y_{i,j} + \Delta y]$) for finite volume method (respectively finite difference) where $\Delta x > 0$ (respectively Δy) is the space step in the x-direction (resp. y-direction).

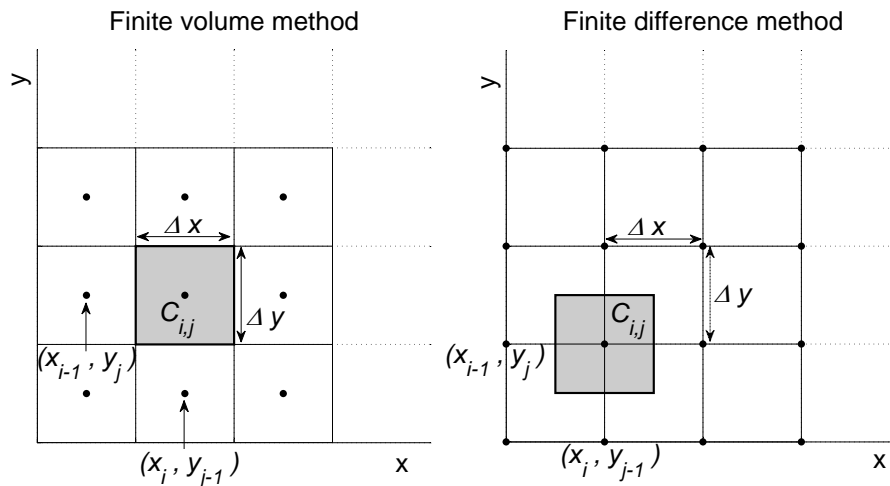


Figure 3: Spatial discretization, comparison between the two numerical methods: Volume Finite and Difference Finite.

2.2.1 Shallow water with a finite volume scheme (SW/FV)

Here we use an object oriented code in $C++$ (free software and GPL-compatible license CeCILL-V2¹). Source code available at <http://www.univ-orleans.fr/mapmo/soft/FullSWOF/> solving the shallow water system with a well balanced finite volume method, it is called FullSWOF_2D (for Full Shallow Water equations for Overland Flow in 2D) and was developed and partially supported by the ANR project METH-ODE² see [16, 54, 21].

¹<http://www.cecill.info/index.en.html>

²project ANR-07-BLAN-0232 granted by the French National Agency for Research

We consider the Shallow Water system (1)-(2)-(3) and introduce four vectors to write it in a compact form:

$$U = \begin{pmatrix} h \\ hu \\ hv \end{pmatrix}, \quad F(U) = \begin{pmatrix} hu \\ hu^2 + \frac{g}{2}h^2 \\ huv \end{pmatrix},$$

$$G(U) = \begin{pmatrix} hv \\ huv \\ hv^2 + \frac{g}{2}h^2 \end{pmatrix} \text{ and } B(U) = \begin{pmatrix} R - I \\ -gh(S_{0_x} + S_{f_x}) \\ -gh(S_{0_y} + S_{f_y}) \end{pmatrix}.$$

U is the vector of conservative variables; F and G are the flux vectors in each horizontal direction; B corresponds to the source term and depends on U because of bed friction. With these notations, the Shallow Water system, expressed in the differential conservative form, has the following expression:

$$\frac{\partial U}{\partial t} + \frac{\partial F(U)}{\partial x} + \frac{\partial G(U)}{\partial y} = B(U). \quad (9)$$

We can write the two-dimensional semi-discrete finite volume formulation of system (9):

$$\frac{d}{dt}U_{i,j} + \frac{1}{\Delta x}(F_{i+1/2,j}^* - F_{i-1/2,j}^*) - \frac{1}{\Delta y}(G_{i,j+1/2}^* - G_{i,j-1/2}^*) = S_{i,j}.$$

$U_{i,j}$ is an approximation of the conservative variables U in the cell $C_{i,j}$, $F_{i+1/2,j}^*$ (respectively $G_{i,j+1/2}^*$) the numerical flux at the interface between $C_{i,j}$ and $C_{i+1,j}$, (resp. between $C_{i,j}$ and $C_{i,j+1}$) and $S_{i,j}$ the source term discretization. For the sake of simplicity, we follow the explication only for the one-dimensional case. To obtain a second order accuracy in space, we have reconstructed our variables with a modified ENO linear reconstruction and a minmod slope limiter which is an elementary method to extend accuracy of a finite volume scheme (for more details see [8, 16]). Naturally, one would make it on z and h separately, but in practice one makes it on $z + h$ and h , and deduces z , because it allows to treat correctly the dry/wet interfaces [2]. So, we reconstruct $h + z$ to get $z_{i+1/2-}$ and $z_{i+1/2+}$ the reconstruction of z on each side of the interface $i + 1/2$, in case of inflow or dry soil. Furthermore, it is not so obvious to get a steady state preserving scheme (at rest too, for example a lake at rest), but it is necessary for the result credibility. In order to preserve them we can use schemes which are called well balanced (since Greenberg and Leroux [31]). It consists in choosing a finite volume scheme with the good properties (water height positivity preserving, consistent) depending on the chosen numerical flux. Then a correction is applied to deal properly with the source term, *i.e.* to preserve steady state. The equilibrium or stationary states are given by:

$$\begin{cases} \partial_t h = 0 \\ \partial_t u = 0 \end{cases} \Rightarrow \begin{cases} \partial_x hu = 0 \\ \partial_x (h + z + u^2/g) = 0 \end{cases},$$

which is Bernoulli's law. To simplify we restrict to equilibria nearly at rest ($u \ll \sqrt{gh}$): $u = \text{cst}$, $g(h + z) = \text{cst}$. So $u = 0$ is included. This procedure is called the hydrostatic reconstruction, for more details we refer to [1, 8, 42]. In one-dimensional case, our scheme writes:

$$U_i^{n+1} - U_i^n + \frac{\Delta t}{\Delta x} (F_{i+1/2L}^n - F_{i-1/2R}^n) = \frac{\Delta t}{\Delta x} S_{i,j}^n.$$

Where

$$F_{i+1/2L}^n = F\left(U_{i+1/2L}^n, U_{i+1/2R}^n\right) + \begin{pmatrix} 0 \\ \frac{g}{2}((h_{i+1/2-}^n)^2 - (h_{i+1/2L}^n)^2) \end{pmatrix},$$

$$F_{i-1/2R}^n = F\left(U_{i-1/2L}^n, U_{i-1/2R}^n\right) + \begin{pmatrix} 0 \\ \frac{g}{2}((h_{i-1/2+}^n)^2 - (h_{i-1/2R}^n)^2) \end{pmatrix}.$$

Here, variables indexed by $i_{\pm 1/2R}$ or $i_{\pm 1/2L}$ stand for the result of the second order hydrostatic reconstruction (10). The ones indexed by $i_{\pm 1/2-}$ or $i_{\pm 1/2+}$ result from ENO modified (Essentially Non Oscillatory) type reconstruction. The states $U_{i+1/2L}$ and $U_{i-1/2R}$ have the following expression:

$$\begin{cases} h_{i+1/2L} = \max(0, h_{i+1/2-} + z_{i+1/2-} - \max(z_{i+1/2-}, z_{i+1/2+})), \\ h_{i-1/2R} = \max(0, h_{i-1/2+} + z_{i-1/2+} - \max(z_{i-1/2-}, z_{i-1/2+})), \\ U_{i+1/2L} = (h_{i+1/2L}, h_{i+1/2L}u_{i+1/2-})^t, \\ U_{i-1/2R} = (h_{i-1/2R}, h_{i-1/2R}u_{i-1/2+})^t. \end{cases} \quad (10)$$

Moreover to preserve the consistency, a cell centered source term is added:

$$S_i^n = \begin{pmatrix} R_i^n - I_i^n \\ \frac{g}{2}((h_{i-1/2+}^n)^2 - (h_{i+1/2-}^n)^2)(z_{i+1/2-} - z_{i-1/2+}) \end{pmatrix}$$

As numerical flux, we use the HLL flux [33]:

$$F(U_l, U_r) = \begin{cases} F(U_l), & \text{if } \sigma_1 > 0, \\ \frac{\sigma_2 F(U_l) - \sigma_1 F(U_r)}{\sigma_2 - \sigma_1} + \frac{\sigma_1 \sigma_2}{\sigma_2 - \sigma_1} (U_r - U_l), & \text{if } \sigma_1 < 0 < \sigma_2, \\ F(U_r), & \text{if } \sigma_2 < 0. \end{cases}$$

Where,

$$\sigma_1 = \inf_{U=U_l, U_r} \inf_{j=\{1,2\}} \lambda_j(U), \quad \sigma_2 = \sup_{U=U_l, U_r} \sup_{j=\{1,2\}} \lambda_j(U)$$

and $\lambda_1 = u - \sqrt{gh}$, $\lambda_2 = u + \sqrt{gh}$ are the eigenvalues of the jacobian of the system.

For the friction law, we chose the semi-implicit treatment because of its stability and preservation of steady states at rest. For more details, refer to [10]. For the Darcy-Weisbach's friction law, the equation (6) implies the following expression for the discharge $q_{x,y}$, where $q_x = hu$, $q_y = hv$ and $|q| = \sqrt{q_x^2 + q_y^2}$:

$$q_{i,x,y}^{n+1} = \frac{\hat{q}_{i,x,y}^{n+1}}{1 + \Delta t f \frac{|\hat{q}_{i,x,y}^{n+1}|}{8(h_i^{n+1})^2}}.$$

For the Manning's friction law, the expression is obtained thanks to the equation (5). To finish, we use a TVD second order Runge Kutta method (Heun) in order to obtain the second-order accuracy in time. We can write our scheme (2.2.1) under the form :

$$U^{n+1} = U^n + \Delta t \Phi(U^n),$$

and we obtain a second-order scheme in time and space as follow:

$$\begin{aligned}\hat{U}^{n+1} &= U^n + \Delta t \Phi(U^n), \\ \hat{U}^{n+2} &= \hat{U}^{n+1} + \Delta t \Phi(\hat{U}^{n+1}), \\ U^{n+1} &= \frac{U^n + \hat{U}^{n+2}}{2}.\end{aligned}$$

For more details about this scheme see [8, 2, 42, 16].

2.2.2 Shallow Water with a finite difference scheme (SW/FD)

An other method to solve the two-dimensional unsteady water flow equations is the finite difference MacCormack scheme [39]. Until now, it is the most used and the most “famous” for hydrological applications because of its simplicity and robustness. The finite difference methods are all based on Taylor developments of differentiable and continuous functions. When space step and time step are small, expansions are close to the exact values. We have to solve the matrix formulation (9) with the variables defined above.

The MacCormack scheme with finite-difference consists in a two steps process (predictor-corrector) which allows second-order accuracy. With the same notations, we can define the two steps as follow:

Predictor

We calculate U at time $t + \Delta t$ using known values at time t and forward differences.

$$[U_{i,j}^{n+1}]_p = U_{i,j}^n + \Delta t \left(B(U_{i,j}^n) - \frac{F(U_{i+1,j}^n) - F(U_{i,j}^n)}{\Delta x} - \frac{G(U_{i,j+1}^n) - G(U_{i,j}^n)}{\Delta y} \right),$$

Corrector

$$\left(\frac{\partial U_{i,j}}{\partial t} \right)_{cor}^{n+1} = B([U_{i,j}^{n+1}]_p) - \frac{F([U_{i,j}^{n+1}]_p) - F([U_{i-1,j}^{n+1}]_p)}{\Delta x} - \frac{G([U_{i,j}^{n+1}]_p) - G([U_{i,j-1}^{n+1}]_p)}{\Delta y}.$$

Then, we have the solution at time step $n + 1$ with an average between the predictor and corrector step.

$$U_{i,j}^{n+1} = \frac{U_{i,j}^n + [U_{i,j}^{n+1}]_p}{2} + \frac{\Delta t}{2} \left(\frac{\partial U_{i,j}}{\partial t} \right)_{cor}^{n+1}.$$

Moreover, in that model we use a dissipation term in order to reduce oscillations near discontinuities [14].

$$\frac{\partial U}{\partial t} + \frac{\partial F(U)}{\partial x} + \frac{\partial G(U)}{\partial y} - \left(\Delta x^2 \frac{\partial}{\partial x} \left(D(x, y) \frac{\partial U}{\partial x} \right) + \Delta y^2 \frac{\partial}{\partial y} \left(D(x, y) \frac{\partial U}{\partial y} \right) \right) = B(U).$$

The coefficient $D(x, y)$ (or artificial viscosity), has to be positive and takes its values in $[0, 10]$. Here we have chosen to take it constant and once the above equation rewritten, we solve by a centred scheme the following equation:

$$\frac{\partial U}{\partial t} + \frac{\partial}{\partial x} F^*(U) + \frac{\partial}{\partial y} G^*(U) = B(U),$$

with $F^*(U) = F(U) - D\Delta x^2 \frac{\partial U}{\partial x}$, and $G^*(U) = G(U) - D\Delta y^2 \frac{\partial U}{\partial y}$.

For the friction law, in this code we choose the semi-implicit treatment for the

same reasons as for the previous scheme (stability and preservation of steady states at rest) and for more details refer to Bristeau and Coussin [10]. Moreover, in the case of very small water depth (between $h_{fix} = 10^{-4}$ m and zero), we approximate the velocity of a very thin water film using the steady state kinematical wave equation and a linear interpolation function (see [22]). So we compute velocities using following formulations:

$$\begin{aligned} \text{Manning: } u &= \frac{h^{4/3}}{h_{fix}^{2/3}} \sqrt{|S_{0x}|/K} \quad , \quad v = \frac{h^{4/3}}{h_{fix}^{2/3}} \sqrt{|S_{0y}|/K}, \\ \text{Darcy-Weisbach } u &= \frac{h}{h_{fix}} \sqrt{8g|S_{0x}|h_{fix}/f} \quad , \quad v = \frac{h}{h_{fix}} \sqrt{8g|S_{0y}|h_{fix}/f}. \end{aligned}$$

2.2.3 Kinematic Wave with a finite volume method (KW/FV)

Here, we use a finite-volume resolution with a standard upwind scheme. System (9) reduces in the following form

$$\begin{aligned} U &= \begin{pmatrix} h \\ 0 \\ 0 \end{pmatrix}, \quad F(U) = \begin{pmatrix} hu \\ 0 \\ 0 \end{pmatrix}, \\ G(U) &= \begin{pmatrix} hv \\ 0 \\ 0 \end{pmatrix}, \quad B(U) = \begin{pmatrix} R - I \\ -gh(S_{0x} + S_{fx}) \\ -gh(S_{0y} + S_{fy}) \end{pmatrix}. \end{aligned} \quad (11)$$

We obtain a system which is easier to solve.

$$\frac{\partial U}{\partial t} + \frac{\partial F(U)}{\partial x} + \frac{\partial G(U)}{\partial y} = B(U). \quad (12)$$

We compute the discharge q_x and q_y ($q_x = hu$ and $q_y = hv$) thanks to the equality between friction and slope term (see (7)-(8) in 2.1.3). Then, we can apply the upwind scheme to obtain the water height at the time step $n + 1$ in the cell $C_{i,j}$:

$$h_{i,j}^{n+1} = \begin{cases} h_{i,j}^n - \Delta t \left(\frac{q_{x_{i+1,j}}^{n+1} - q_{x_{i,j}}^{n+1}}{\Delta x} + \frac{q_{y_{i,j+1}}^{n+1} - q_{y_{i,j}}^{n+1}}{\Delta y} \right) + R - I & \text{if } u, v < 0, \\ h_{i,j}^n - \Delta t \left(\frac{q_{x_{i,j}}^{n+1} - q_{x_{i-1,j}}^{n+1}}{\Delta x} + \frac{q_{y_{i,j}}^{n+1} - q_{y_{i,j-1}}^{n+1}}{\Delta y} \right) + R - I & \text{if } u, v > 0, \\ h_{i,j}^n - \Delta t \left(\frac{q_{x_{i+1,j}}^{n+1} - q_{x_{i,j}}^{n+1}}{\Delta x} + \frac{q_{y_{i,j}}^{n+1} - q_{y_{i,j-1}}^{n+1}}{\Delta y} \right) + R - I & \text{if } u < 0, v < 0, \\ h_{i,j}^n - \Delta t \left(\frac{q_{x_{i,j}}^{n+1} - q_{x_{i-1,j}}^{n+1}}{\Delta x} + \frac{q_{y_{i,j+1}}^{n+1} - q_{y_{i,j}}^{n+1}}{\Delta y} \right) + R - I & \text{if } u > 0, v > 0. \end{cases}$$

For the Kinematic Wave model, we can notice limitations with this physical model. Indeed, if there is no topography variation, we obtain a null discharge, whereas it is possible to have overland flow on flat land. This represents the limits of the Kinematic Wave model. Moreover, it is impossible to take a configuration without friction, indeed $S_0 = S_f$ does not allow it.

2.2.4 Kinematic Wave with a finite difference scheme (KW/FD)

With the formulation (12) and vectors defined at (11), we can solve the system by finite difference method. In that model, we use a central scheme and as previously we calculate discharges q_x and q_y ($q_x = hu$ and $q_y = hv$) thanks to the equality between friction and slope term (see (7)-(8) in 2.1.3). So we have the following water height at the time step $n + 1$ in the cell $C_{i,j}$:

$$h_{i,j}^{n+1} = h_{i,j}^n - \Delta t \left(\frac{q_{x_{i+1,j}}^{n+1} - q_{x_{i-1,j}}^{n+1}}{2 \cdot \Delta x} + \frac{q_{y_{i,j+1}}^{n+1} - q_{y_{i,j-1}}^{n+1}}{2 \cdot \Delta y} \right) + R - I.$$

3 Test cases

The four models presented above are compared on different test cases. The first test case is the preservation of a steady state at rest, it is important in the sense that it means, for example, a ponding water conservation. The second is a comparison on the rising hydrograph thanks to a “naive” analytical solution (introduced in [17, 18]), here we suppose the soil impermeable and only frictions and rainfall are considered. The third, which is decomposed into two configurations, has been chosen in order to represent a realistic configuration which takes into consideration the rainfall, the friction and the infiltration. In a last time an analytical test case has been simulated. As we aim at modelling run-off, it is a main point that the model is able to cope with inflow on dry soil, *i.e.* with dry/wet interfaces.

3.1 Preservation of steady state at rest

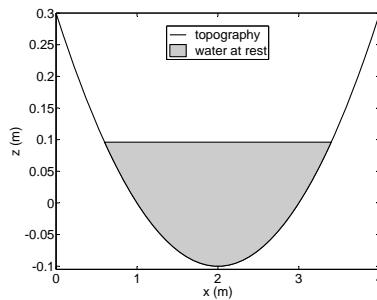


Figure 4: “Preservation of steady state at rest” test case: parabola with initial water at rest inside.

The initial configuration takes place inside a parabola of revolution (13) on the domain $[0, 4 \text{ m}] \times [0, 4 \text{ m}]$ (see Figure 4), we impose a water height such as $h + z = 0,2$ inside the parabola. Here, we assume that the soil is impermeable and we consider a small friction coefficient, even if it is impossible for KW model to cope with (friction coefficient for the Manning’s law equal to 0,01). Indeed, for KW model the motion equation represents the equality ($S_0 = S_f$), so a null friction engenders a zero slope whatever the configuration, it is why simulations

without friction cannot be modelled by KW. The topography is given by:

$$z(X, Y) = -H_0(1 - X^2 + Y^2). \quad (13)$$

3.2 Rising hydrograph

It takes place on a plane with a slope of 5% in one direction of space, represented Figure 5, with a friction coefficient for the Darcy-Weisbach law ($f = 0.25$). Here we do not consider the infiltration process, *i.e.*: we assume that the soil is impermeable. We apply, uniformly on all the domain, a rainfall intensity R as follows:

$$R(t) = \begin{cases} 50 \text{ mm.h}^{-1} & \text{if } t \in [0, 125], \\ 0 \text{ mm.h}^{-1} & \text{otherwise.} \end{cases}$$

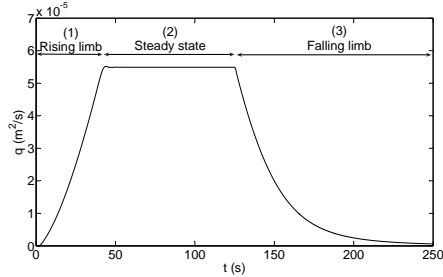
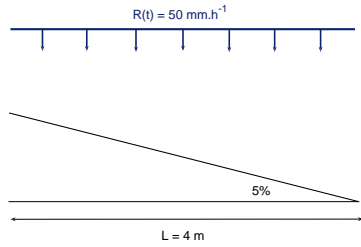


Figure 5: “Rising hydrograph” test initial configuration. Figure 6: Runoff hydrograph for an impermeable configuration.

Observing that the hydrograph is composed of three phases (see Figure 6): (1) at the beginning of the rainfall event a non-steady state that we will call “rising limb”, (2) a steady-state and to finish (3) a non-steady state which represents the drying. A “naive” analytical solution can be computed explicitly for the two first steps. So we can obtain a “naive” solution and calculate the water height profile and the discharge downstream and in the middle of our plane. To have more explications on the “naive” solution refer to [16, 17, 18].

3.3 Hillslope 1 and 2

We consider a little hillslope with a quarter of paraboloid shape on the domain $[0, 20 \text{ m}] \times [0, 20 \text{ m}]$, its coefficients concerning infiltration and friction process, and a rainfall event. The rainfall intensity $R(t)$ is considered uniform on all the domain and takes the following values:

$$R(t) = \begin{cases} 35 \text{ mm.h}^{-1} & \text{if } t \in [0, 720], \\ 60 \text{ mm.h}^{-1} & \text{if } t \in]720, 1080], \\ 0 \text{ mm.h}^{-1} & \text{otherwise.} \end{cases}$$

With this rainfall event, we have chosen to take two sorts of configurations: firstly, one with uniform soil parameters on the paraboloid with the soil properties of area 1 (“Hillslope 1”) and secondly, one with three groups of soil parameters (area 2-3-4) divided into five plots (“Hillslope 2”). Figure 7 and Table 1

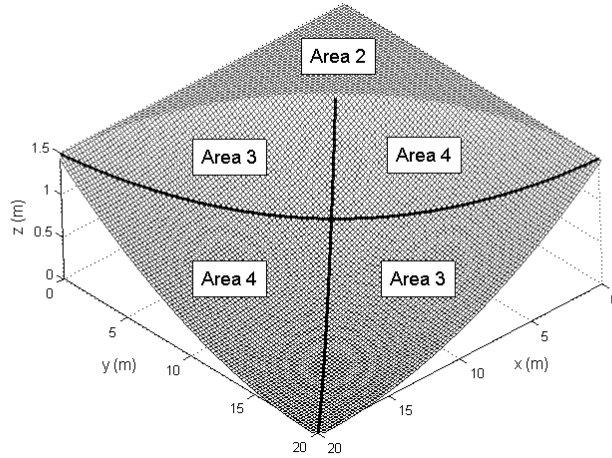


Figure 7: “Hillslope 1 and 2”: initial topography and distribution of soil parameters in case of configuration 2.

present respectively the initial configuration with the four different areas, and the values taken by the soil parameters.

	$K_s(\text{m}\cdot\text{s}^{-1})$	$h_f(\text{m})$	$\theta_s - \theta_i$	K
area 1	$3\cdot 10^{-7}$	$2.3\cdot 10^{-2}$	0.5	0.035
area 2	$1\cdot 10^{-7}$	$3.5\cdot 10^{-2}$	0.5	0.025
area 3	$3\cdot 10^{-7}$	$2.3\cdot 10^{-2}$	0.5	0.015
area 4	$8.4\cdot 10^{-6}$	$6.1\cdot 10^{-2}$	0.5	0.035

Table 1: “Hillslope 1 and 2” test cases: values of main parameters for different soils considered.

3.4 Analytical solution: Thacker’s axisymmetrical solution

The initial configuration takes place, as in “Steady state at rest” test case, in the parabola of revolution (13) on the domain $[0, 4 \text{ m}] \times [0, 4 \text{ m}]$, water height and velocities are given by a system (14) which represents the analytical solution as functions of space and time, see [61]. For the initial conditions, we take them at time $t = 0 \text{ s}$, and the initial surface elevation shaped as an inverse parabola of revolution and velocities are null (see Figure 8). However, frictions are not included in the model, so there is no energy dissipation and the solution is a radially symmetrical oscillating paraboloid (with perpetual motion). But it is impossible for the kinematic wave to have a such configuration because of the motion equation which represents equality between the friction

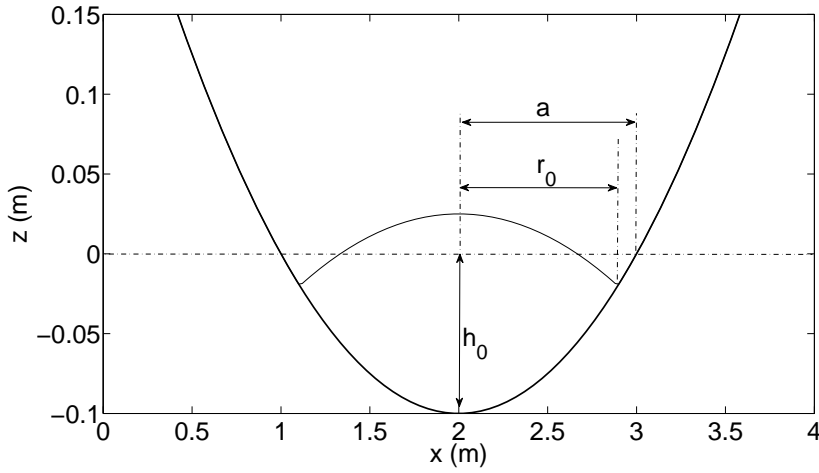


Figure 8: “Thacker’s axisymmetrical solution” test case: initial configuration and conditions.

term and the gradient slope. Indeed, a friction term equal to zero generates, whatever the configuration, a slope gradient equal to zero what it is wrong and so, such test cases cannot be simulated by KW model. Moreover, testing with the MacCormack resolution it appears that the model stops after the first periode. Therefore we have added a friction term in order to test the three models, the friction can be associated to energy dissipation and it slows the motion flow and consequently softens oscillations. It allows MacCormack resolution model to run smoothly until the end of simulation. The parabola and curved solution (see [61, 42]) is given by

$$\left\{ \begin{array}{l} h(r, t) = H_0 \left(\frac{\sqrt{1 - D^2}}{1 - D \cos(\omega t)} - 1 - r^2 \left(\frac{1 - D^2}{(1 - D \cos(\omega t))^2} - 1 \right) \right), \\ u = \frac{1}{1 - D \cos(\omega t)} (0.5wXD \sin(\omega t)), \\ v = \frac{1}{1 - D \cos(\omega t)} (0.5wYD \sin(\omega t)), \\ r = X^2 + Y^2. \end{array} \right. \quad (14)$$

Where the frequency ω is : $\omega = \sqrt{8gh_0/a^2}$, $D = (a - r_0^2)/(a + r_0^2)$, $X = x - 2$, and $Y = y - 2$. In this test, we have used as values $a = 1$, $r_0 = 0.8\text{m}$ and $h_0 = 0.1$ m. Moreover, in the case with friction term considered as explained previously (in this case, there is no analytical solution), we have taken a friction coefficient for the Manning’s law equal to 0,01.

4 Results and discussion

4.1 Preservation of steady state at rest

The results of the two numerical codes based on the KW model, KW/FD and KW/FV, are not represented here. Indeed, their results present important in-

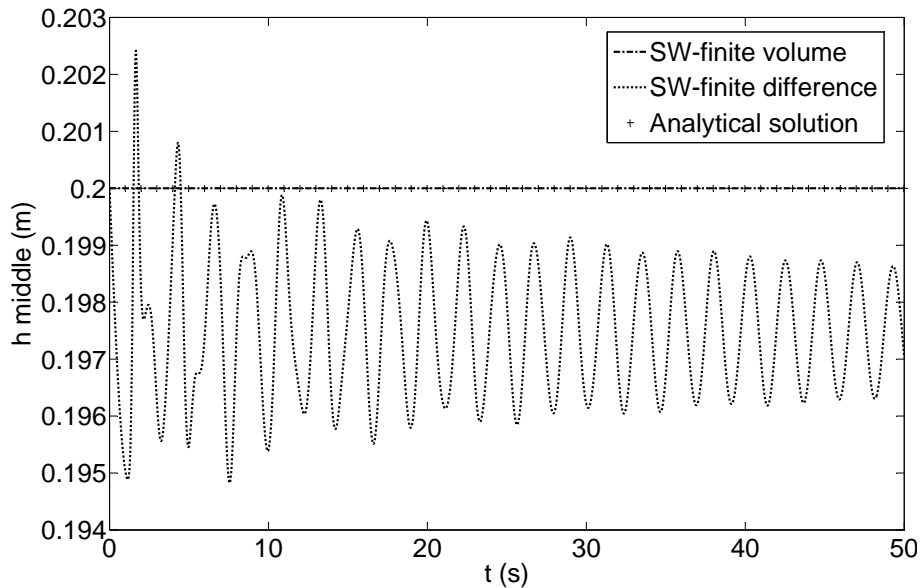


Figure 9: “Preservation of steady state at rest” test case: evolution of the middle water elevation.

stabilities, and from the first time steps their simulated water depths rise rapidly (water volume gain), then oscillate, and become infinite. In this case, the resolution method is not calling into question, but the equation system, KW model, seems not to cope with complex topography, as here a bassin with a parabola of revolution. Figure 9 represents the water height at the middle point of the parabola, we can observe that for the SW/FV the water height is constant and equal to the initial water height while the SW/FD water height fluctuates around a value which is not the analytical solution. We can conclude that, because of its oscillations, the SW/FD is not a stable scheme, and moreover, as its simulated water depth is smaller than the theoretical one, we can deduce that SW/FD is not a conservative scheme. Furthermore, calculating the volume conservation, one can observe that SW/FV has a perfect conservation, whereas SW/FD loses few water. This test case is important for an hydrologic code, it allows to know if the scheme preserves these steady states at rest to represent the formation of ponding water for example.

4.2 Rising hydrograph

Figures 10 and 11 present, for the four numerical codes and the “naive” analytical solution, the discharges at two locations: the outlet (Figure 10) and the middle plan point (Figure 11). Indeed, during a uniform rainfall event the rainfall hydrograph is composed of three steps (see Figure 6): (1) a first one which is called the rising limb, (2) a second one which is an equilibrium state, and (3) a last one the falling limb. For the two firsts steps, as we simulate a constant and uniform rainfall on the domain, it is possible to calculate a “naive”

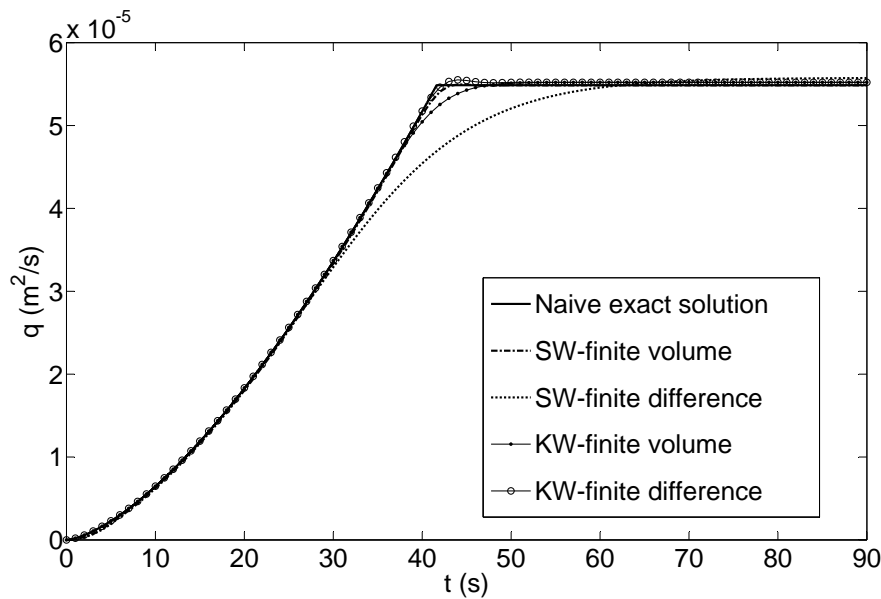


Figure 10: “Rising hydrograph” test case: comparison between rainfall hydrogram computed with four different methods and “naive” exact solution, at the outlet.

analytical solution of this problem [17, 18]. During the rising limb, KW/FD, KW/FV, SW/FV give a good estimation of the analytical discharge at the middle plan point, like KW/FD and KW/FV at the outlet point whereas SW/FV underestimates slightly the discharge ($\leq 1\%$). While the three codes (KW/FD, KW/FV and SW/FV) give water depths very close to the analytical solution along the rising limb, we observe that SW/FD has an evolutive behavior at the two points (middle one and outlet one). Indeed, Figures 10 and 11 show that SW/FD slightly underestimates the analytical discharge at the beginning of the event, then improves itself during few seconds, but highly underestimates after 34 seconds at the middle point, and 62 seconds at the outlet point (13%). Concerning the second step of the hydrograph (equilibrium state), note that even if the discharges estimated by KW/FD and SW/FD seem to become constant, their values are gradually varying at the two observation locations (middle and outlet) and therefore do not reach an equilibrium state. Besides, we can remark that the KW/FD and SW/FD simulated discharges overestimate slightly the analytical one at the outlet point (less than 1%), this observation is in the same order at the middle plan point for KW/FD, but becomes more important for SW/FD (11%). Concerning SW/FV and KW/FV, they reach an equilibrium state for the two observation locations, but are approximately 10 seconds late compared with the analytical. Another point is that, whereas SW/FV estimates a stable discharge very close to the theoretical one at the two observation locations, KW/FV obtains a low overestimation (1%). Additionally, calculating volume conservation, we can see that it is better for KW/FV simulation (0% of loss) but remains good for KW/FD and SW/FV (1% of loss for KW/FD and 1%

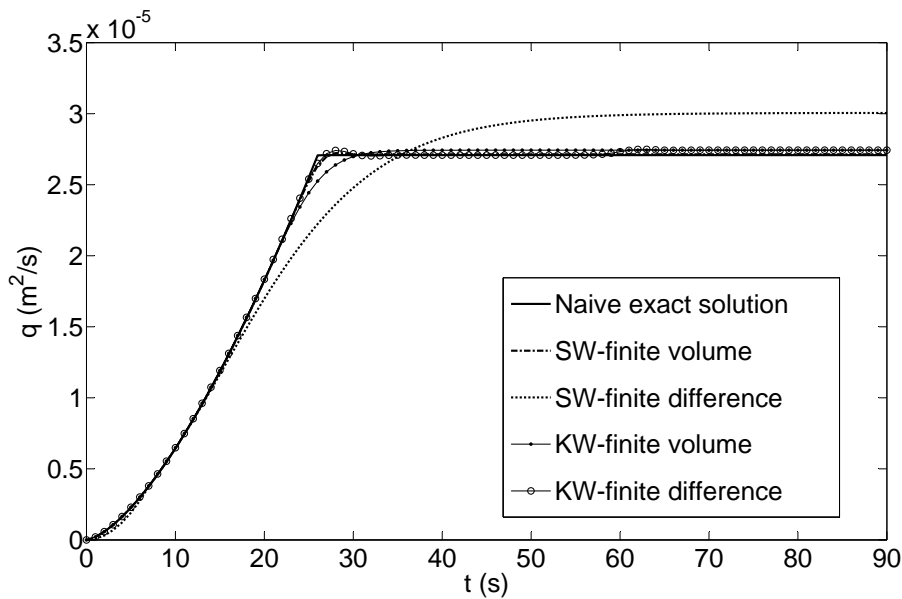


Figure 11: “Rising hydrograph” test case: comparison between rainfall hydrograph computed with four different methods and “naive” exact solution, in the middle of plane.

of excess for SW/FV), and admissible for SW/FD (2.4% of loss). Eventually, regarding the errors made on the water depth, classifying the codes by growing errors, first we have SW/FV (0.015), then KW/FV (0.019), KW/FD (0.022), and SW/FD (0.1).

4.3 Hillslope 1 and 2

Contrary to the other test cases, we do not have an analytical solution for “Hillslope 1 and 2” test cases, so we just can make comparisons between the results of the four numerical codes. Figure 12 shows the discharge simulated at outlets for the configuration 1, that is to say on the hillslope with homogeneous soil surface parameters (“Hillslope 1”). Firstly we can observe two discharge stages which represent the two parts of the rainfall event and besides, owing to infiltration, the discharge does not necessarily reach a steady state and becomes constant. An important point is that the discharge shapes seem to have the same form in function of the model. Even if they do not simulate the same values, the chosen model allows one to determine the expected form of hydrograph. We can notice that SW/FD overestimates significantly the discharge in comparison with the three other codes, around 150% for the first hydrograph stage and around 140% for the second stage. During the first stage of the hydrograph, SW/FV and KW/FV have their discharge curves which intersect staying very close together (less than 2%), whereas the KW/FD simulated discharge takes slightly higher values (less than 6%). Moreover, during the second stage of the hydrograph, we observe a change of curves relation: SW/FV and KW/FD intersect

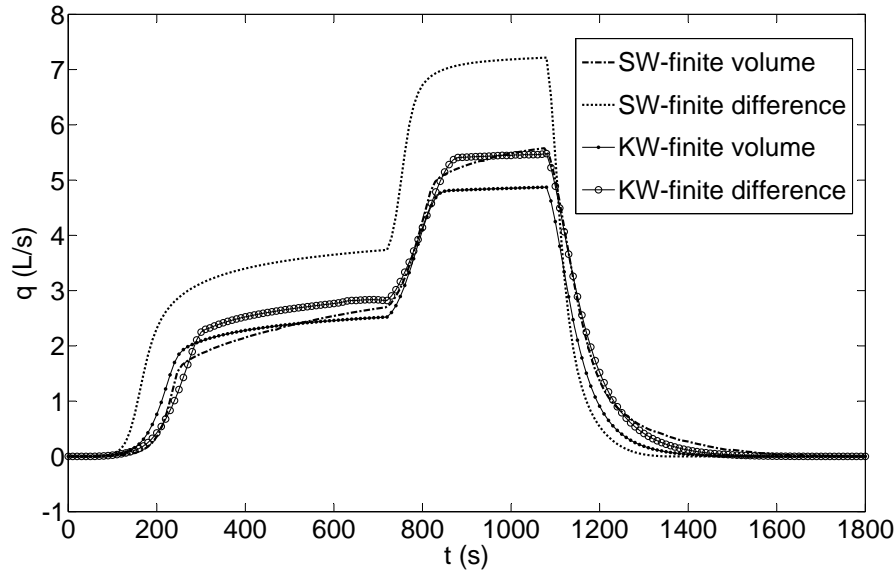


Figure 12: “Hillslope 1”: comparison between the four different methods, for the runoff discharge (q) at the outlets.

and are closed together, whereas KW/FV gives discharge values approximately 13% smaller than SW/FV and KW/FD. Concerning the codes ability to flow, comparing their runoff coefficient (defined as the total volume of runoff divided by the total volume of rainfall), we remark that KW/FV and KW/FD give relatively similar coefficients, respectively 73.8% and 72.5%, whereas SW/FV has the smallest one 67.8%, and SW/FD simulates the most important runoff with 89%. Regards to volume conservation, we can note that KW/FV has a perfect conservation (0% of loss), and SW/FV a loss of about 3%, whereas KW/FD an excess of about 7% and SW/FD an excess of about 14%. At this stage, we can deduce that for this uniform configuration, SW/FD generates more runoff, but in the same time it is the less conservative. So disregarding SW/FD, we can state that the Kinematic Wave produces more runoff more than Shallow Water. Moreover, concerning numerical resolution property, Finite Difference is a less conservative scheme than Finite Volume. Figure 13 represents the discharge at the outlet for the configuration 2, that is to say for an infiltration coefficient repartition not uniform (“Hillslope 2”). In this test case, we do not represent the SW/FD results because it significantly and abnormally overestimates predicted water volume, it is totally nonconservative on this configuration and its results cannot be treated. We may note that the infiltration parameter repartition has a major influence on the ponding prediction, in fact, we have a significant difference between the discharge simulated by SW/FV and KW/FV. SW/FV discharge is approximately three times greater than KW/FV one. Moreover, comparing the runoff coefficients we observe that, contrary to “Hillslope 1” test case with uniform soil parameters, the code generating the most of runoff

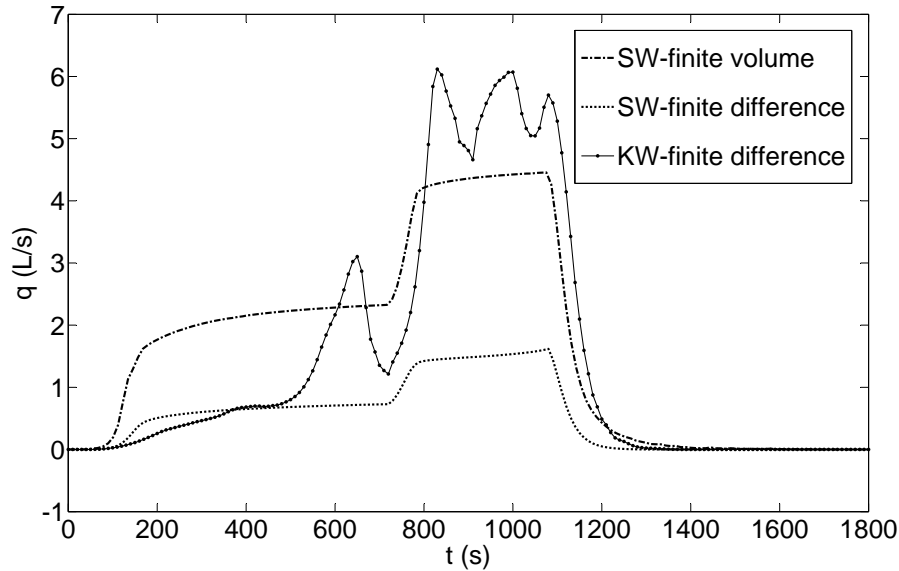


Figure 13: “Hillslope 2”: comparison between the three different methods, for the runoff discharge (q) at the outlets.

is SW/FV with 57.5%, then KW/FD with 47.3%, and at last KW/FV which coefficient is only 32.7% (representing less than half of the “Hillslope 1” coefficient). We can also observe a significant difference for the discharge behaviour between KW/FD and the two other codes, SW/FV and KW/FV, which have a similar profile composed of two discharge stages, due to the two parts of rainfall event and which begin around the same time. For KW/FD, peak of runoff seems to be numerical artefact, consequence of the non-stability of the scheme and not a physical result. With regard to the volume conservation, in this test case it appears that KW/FD is not conservative because of more than 37% of water volume excess. The two others have a good conservation (0% of loss for KW/FV and less than 2% of loss for SW/FV). Once again, we can deduce that Finite Difference is a non-conservative scheme, but contrary to “Hillslope 1”, we notice that the KW/FV promotes the infiltration and undervaluates the discharge and more precisely the velocities. Indeed, the comparison between the two configurations, “Hillslope 1” and “Hillslope 2” during the first stage of the hydrograph, shows that the discharges decrease by 400% for KW/FV, and only 112% for SW/FV. As for the second stage, whereas the decreasing discharge predicted by KW/FV is close to 300%. The decreasing calculated for the SW/FV discharges is only 111%. Besides, we remark a higher difference for the velocities, we can therefore deduce the underestimation of KW/FV discharges are due to the underestimation of the velocities and not the water depths.

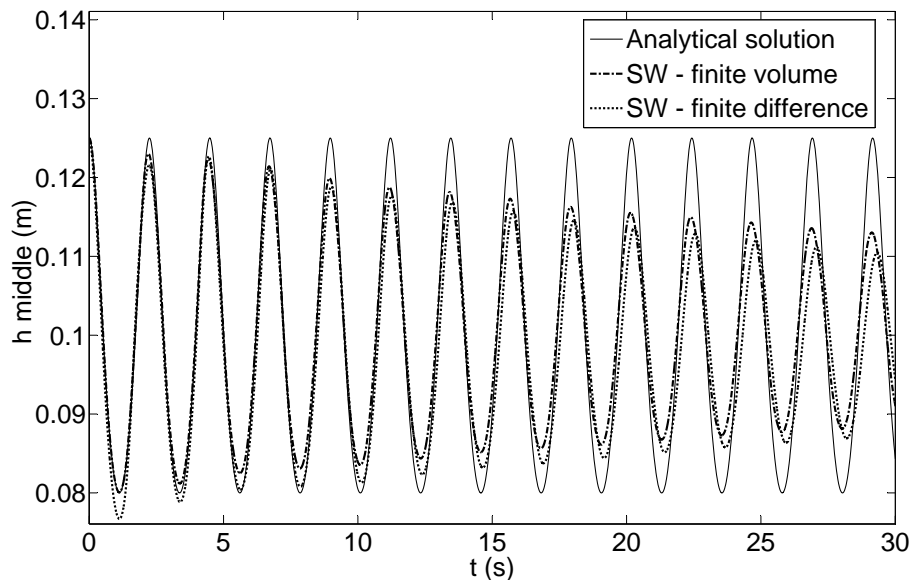


Figure 14: “Thacker’s axisymmetrical solution” test case: comparison between middle water elevation computed with two different methods and analytical solution.

4.4 Thacker’s axisymmetrical solution

Firstly, motivations of this test case is that it allows one to impose dry/wet interfaces and to know if the model can cope with such phenomena, which may often appears with rainfall overland flows. Using this test case without friction, SW/FD stops after the first period. Moreover, for KW model it is impossible to simulate the test case without friction because of the motion equation ($S_0 = S_f$) which generates, if the friction term is null, a slope gradient always equals to zero. Consequently, we have added a friction term, which has the same effect on the response that a numerical diffusion, *i.e.* it slows oscillations down and therefore softens instabilities, a difference regarding the oscillation depth between exact and modelling solution is expected. But here KW/FV and KW/FD results are not represented owing to important instabilities making the results incoherent with extremely high and low values. As for the first test case, KW does not manage to simulate on such complex topography. Figure 14 presents the comparison of the water height evolution at middle point of parabola, between the analytical solution and the different codes. We can see the damping of water height amplitude increasing with time for the three results, damping is greater for SW/FD and smaller for SW/FV without friction (as expected). Moreover, SW/FV conserves the same period as the analytical solution, whereas SW/FD creates a gap as soon as the second period. In figure 15, we focus on the run-up and run-down phenomena, it shows the water height profile for different instants between the time $t = 3T/2$ and $t = 3T$, at the same time for the codes and the analytical solution. Here we notice that

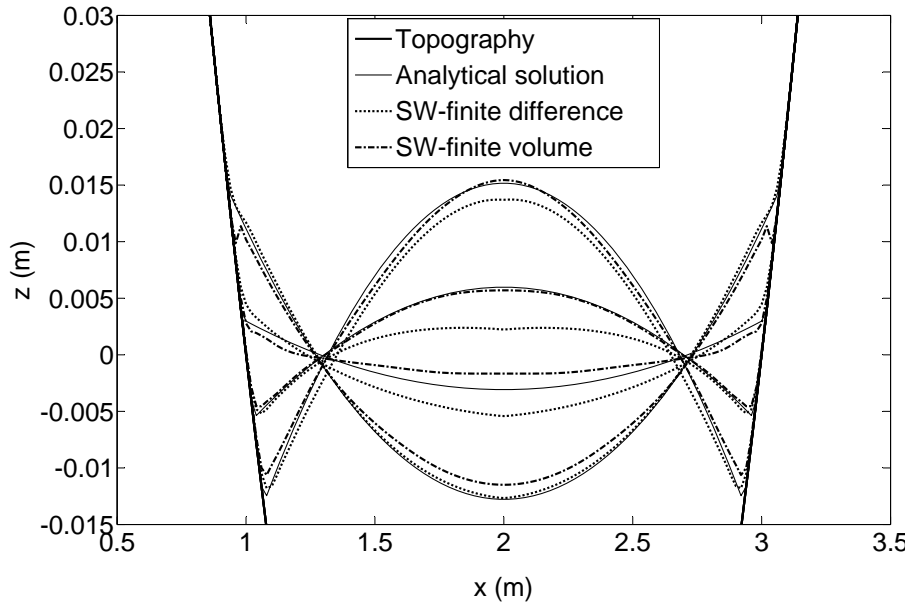


Figure 15: “Thacker’s axisymmetrical solution” test case: comparison between two different methods and analytical solution for the surface elevation. Zoomed profiles of water depth are plotted for different values of time between $t = 3T/2$ and $t = 3T$.

the difference between analytical solution and simulation results is more significant and important at dry/wet interfaces in the case of SW/FD resolution. We can see that SW/FV loses less amplitude for maximum surface elevation than SW/FD, and this tendency is in reverse order for the minimum surface elevation. So even if here SW/FD results are not really different to SW/FV results, SW/FD is not able to simulate this test case without friction, this coming from the fact that no friction generates instabilities and it does not cope with.

4.5 Discussion

Table 2 presents a result synthesis of the five simulated test cases. This table underlines the pros and cons of each numerical code for different outputs, as the volume conservation, the runoff coefficient... Firstly, we remark that the Kinematic Waves (KW) model, with Finite Difference (FD) resolution or Finite Volume (FV) resolution, does not allow to simulate test cases on parabola topography. Indeed, for “Steady state” and “Thacker” test cases which take place in a parabola of revolution, KW/FD and KW/FV obtain incoherent outputs, and this even refining the mesh or decreasing the gradient slope. Looking the KW model equations we remark that, contrary to Shallow Water (SW), KW implies a discharge or a depth-average velocity of which components are independent. Moreover, regarding the volume conservation in Table 2, SW/FD is the less conservative code for the set of the five test cases (following by KW/FD), it has the highest loss of water. The Finite Volume method gives therefore a

	KW Finite difference	KW Finite volume	SW Finite difference	SW Finite volume
“Steady state” Volume conservation Error on water depth (discharge)	X 0.022 (0.027)	X 0.019 (0.024)	-0.15% 0.099 (0.124)	0% 0.015 (0.016)
“Rising hydrograph” Volume conservation Error on water depth (discharge)	+1.07% 0.022 (0.027)	0% 0.019 (0.024)	-2.38% 0.099 (0.124)	-1% 0.015 (0.016)
“Hillslope 1” Volume conservation Runoff coefficient	+7.64% 73.81%	0% 72.50%	+14.35 89.00%	-3.18% 67.82%
“Hillslope 2” Volume conservation Runoff coefficient	+37.54% 47.30%	0% 32.66%	X X	-1.48% 57.51%
“Thacker” Volume conservation Error on water depth (discharge)	-99.98% X	-99.97% X	-0.32% 0.074	0% 0.058 (0.004)

Table 2: Result synthesis of the five test cases for the four numerical codes, **X** is for model crash.

better conservation, that is expected, because the scheme is conservative by construction. Contrary to SW/FD, the code giving the best volume conservation is KW/FV. Indeed, for the three test cases where KW/FD gives coherent (or physical) results, it has a perfect conservation (0% of loss). However it is not the most accurate, as for instance in “Rising hydrograph” test case, its errors on simulated water depth and discharges are the highest. Concerning runoff coefficients in “Hillslope 1 and 2” test cases, first leaving SW/FD out because its important water volume excess alters the calculated runoff coefficient. We observe that, on the hillslope 1 with homogeneous soil parameters, KW/FD and KW/FV have a runoff coefficient close together (resp. 74% et 73%), whereas SW/FV obtains a lower one (68%). But this reverses in the case of the hillslope 2 with an infiltration repartition not uniform, the highest is the runoff coefficient simulated by SW/FV (58%), whereas for KW/FD its coefficient is more than halved (33%) (here we leave KW/FD out because its water volume excess is so great that it alters the calculation too). As regards the runoff, there is a high difference between the two configurations for the KW/FD and KW/FV. Maybe, given the difference of the infiltration parameter values between “Hillslope 1 and 2”, the runoff coefficient should decrease not so much.

The overall aim of this study is to compare overland flow codes with different complexities (KW/FD, KW/FV, SW/FD, SW/FV) and to underline their efficiency. Firstly, we can say, although KW system is a good model to simulate water runoff, it is not able to cope with configurations without friction because of its motion equation. Indeed, taking a configuration without friction, the equality $S_f = S_0$ (that is to say slope gradient is equal to friction term) of the motion equation implies therefore friction coefficient is equal to 0. But the equations (7) and (8), coming from this equality ($S_f = S_0$), involve thus that velocities and discharges are equal to zero whatever the configuration. Moreover the motion equation implies that, on a topography with a flat slope, the discharges stay equal to zero whatever initial assumption. It means that it is impossible to have a positive discharge on a flat domain which is false and gen-

erates a water pounding on such configurations. So if we want to have runoff on flat domain for KW system, we have to modify resolution system and make some other assumptions. For instance, in “Hillslope 1 and 2” test cases, on the top of the domain (which represents area 2 for “Hillslope 2”) as there is no slope, the water does not stream and stagnate. So, whereas the rest of the domain is dry, area 2 has a water height not insignificant (8 mm for “Hillslope 1” and around 1 cm for “Hillslope 2”). In comparison, for SW/FV at the same time, we obtain an insignificant water height on area 2 (less than 10^{-1} mm).

KW has the advantage of being easy and quick to solve and compute, so for simple test case configurations, it could be sufficient, for instance in “Rising hydrograph” or “Hillslope1” test case, it has proved to be efficient and gives good results with the Finite Volume resolution. However, coupled with Finite Difference method, we obtain a non conservative model and we observe in the synthesis (Table 2) that the less conservative results were simulated with finite difference method. Therefore, we can deduce that KW with FV is an efficient combination for simple test cases. Concerning SW system, it is able to simulate more complex configurations, as well initial soil condition (topography, soil parameters) as imposed flow (steady state, fluvial or torrential flow, hydraulic jump), but with Finite Difference resolution, it becomes unstable and not conservative. Solving with Finite Volume method (with hydrostatic reconstruction) allows to obtain a stable and conservative scheme, besides with FV resolution, we have the possibility to simulate unstructured meshing, so to cope with complex topography or soil parameters distribution. Moreover, SW/FV (with hydrostatic reconstruction) perfectly deals with dry/wet interfaces, as in “Thacker” test case and maybe for rainfall events more realistic (not constant) and which generate more dry/wet processes, SW would be more adapted.

It is not possible to rank first one of this 4 models. Only, we can say that compared to Finite Volume, Finite Difference resolution is less conservative, stable and adapted to cases with complex topographies (because of it requires structured grids). So, even if it can be a more complex method to compute, Finite Volume allows more efficiency and accuracy without adding correction term or other technique. With regard to model choice, it depends on applications we want to simulate. In simple topography applications, KW model could be sufficient, but if we want to model more difficult configurations, or rainfall events generating more dry/wet interfaces, SW system is more adapted. For example in case of erosion problem applications, SW/FV would be more efficient and adapted. Indeed, such applications generate topography variations both at spatial and temporal scale, the erosion process is changing the surface elevation which can become therefore more or less complex. Moreover one of advantage of SW/FV (with hydrostatic reconstruction) is that it does not need to modify equation system, add terms or make some assumptions (for example to preserve water height positivity, to deal with slow velocities. . .) to cope with some encountered problems in hydrological modelling, as dry/wet interfaces, heterogeneous parameters.

5 Conclusion

Finally, the results of this study can be used to advise hydrological or soil erosion model users to optimize their choice of the more adapted code in function of their

objectives. The performance of the different configurations that were tested indicates that for hydrological applications on continuous filled (*i.e.* without pit) Digital Elevation Model (DEM), or for erosion applications where the change of elevation is not explicitly modeled (*i.e.* simple computation of sediment flux from cell to cell), the kinematic wave equations solved with the finite volume method is the best option. However, this combination appears to be limited for discontinuous DEM or for areas with strong spatial heterogeneities. In order to avoid the use of numerical tricks, such as the addition of virtual thin water layer on the simulated domain to prevent the appearance of dry/wet interfaces, we advise the use of the shallow water equations solved with the finite volume method. Indeed, it permits to handle a variety of natural configurations able to meet the demand of the majority of the hydrological or soil erosion applications.

References

- [1] E. Audusse. *Modélisation hyperbolique et analyse numérique pour les écoulements en eaux peu profondes*. PhD thesis, Université Pierre et Marie Curie - Paris VI, 2004, available from: <http://tel.archives-ouvertes.fr/tel-00008047/fr/>.
- [2] E. Audusse, F. Bouchut, M.O. Bristeau, R. Klein, and B. Perthame. A fast and stable well-balanced scheme with hydrostatic reconstruction for shallow water flows. *SIAM J. Sci. Comput.*, 25(6):2050–2065, 2004.
- [3] E. Audusse and M.O. Bristeau. A well-balanced positivity preserving “second-order” scheme for shallow water flows on unstructured meshes. *Journal of Computational Physics*, 206(1):311–333, 2005.
- [4] A.J.C. Barré de Saint Venant. Théorie du mouvement non-permanent des eaux, avec application aux crues des rivières et à l’introduction des marées dans leur lit. *Compte Rendu de l’Académie des Sciences, Paris*, 73:147–154, 1871.
- [5] A. Bermudez and M.E Vazquez. Upwind methods for hyperbolic conservation laws with source terms. *Computers & Fluids*, 23(8), 1994.
- [6] J. Boardman and J. Poesen. *Soil Erosion in Europe: Major Processes, Causes and Consequences*, pages 477–487. John Wiley & Sons, Ltd, 2006.
- [7] J. Boardman, G. Verstraeten, and C. Bielders. *Muddy Floods*, pages 743–755. John Wiley & Sons, Ltd, 2006.
- [8] F. Bouchut. *Nonlinear Stability of Finite Volume Methods for Hyperbolic Conservation Laws and Well-Balanced Schemes for Sources*. Birkhäuser Basel, 2004.
- [9] D.L. Brakensiek and W.J. Rawls. Agricultural management effects on soil water processes. part 2, green ampt parameters for crusting soils. *Transactions of the American Society of Agricultural and Biological Engineers*, 26(6), 1983.
- [10] M.O. Bristeau and B. Coussin. Boundary Conditions for the Shallow Water Equations solved by Kinetic Schemes. Research Report RR-4282, INRIA, 2001. Projet M3N.
- [11] N. Chahinian, R. Moussa, P. Andrieux, and M. Voltz. Comparison of infiltration models to simulate flood events at the field scale. *Journal of Hydrology*, 306, 2005.
- [12] V.T Chow. *Open Channel Hydraulics*. McGraw-Hill College, 1959.
- [13] V.T. Chow, D.R. Maidment, and L.W. Mays. *Applied hydrology*. McGraw-Hill Book Compagny, 1988.
- [14] I. Danaila, M. Postel, P. Joly, and S.M. Kaber. *An Introduction to Scientific Computing. Twelve computational projects solved with Matlab*. Springer, 2007.

- [15] A.P.J. De Roo. The litem project: an introduction. *Hydrological Processes*, 10(8):1021–1025, 1996.
- [16] O. Delestre. *Simulation du ruissellement d'eau de pluie sur des surfaces agricoles*. PhD thesis, Université d'Orléans, 2010, available from: <http://tel.archives-ouvertes.fr/tel-00587197/fr/>.
- [17] O. Delestre, S. Cordier, F. James, and F. Darboux. Simulation of rain-water overland-flow. In *Proceedings of the 12th International Conference on Hyperbolic Problems, University of Maryland, College Park (USA), 2008*, E. Tadmor, J.-G. Liu and A. Tzavaras Eds., *Proceedings of Symposia in Applied Mathematics 67*, Amer. Math. Soc., 537–546, 2009.
- [18] O. Delestre and F. James. Simulation of rainfall events and overland flow. In *Proceedings of X International Conference Zaragoza-Pau on Applied Mathematics and Statistics, Jaca, Spain, september 2008*, *Monografías Matemáticas García de Galdeano*, 2009.
- [19] O. Delestre, C. Lucas, P.A. Ksinant, F. Darboux, C. Laguerre, T.N.T. Vo, F. James, and S. Cordier. SWASHES: a library of shallow water analytic solutions for hydraulic and environmental studies. submitted.
- [20] O. Delestre and F. Marche. A numerical scheme for a viscous shallow water model with friction. *Journal of Scientific Computing*, 48:41–51, 2011.
- [21] M. El Bouajaji. Modélisation des écoulements à surface libre : étude du ruissellement des eaux de pluie. Master's thesis, Université Louis Pasteur, available from: <http://dumas.ccsd.cnrs.fr/dumas-00459336/fr/>, Strasbourg, 2007.
- [22] M. Esteves, X. Faucher, S. Galle, and M. Vauclin. Overland flow and infiltration modelling for small plots during unsteady rain: numerical results versus observed values. *Journal of Hydrology*, 228(3-4):265–282, 2000.
- [23] O. Evrard, C.L. Biellers, K. Vandaele, and B. van Wesemael. Spatial and temporal variation of muddy floods in central belgium, off-site impacts and potential control measures. *CATENA*, 70(3):443–454, 2007.
- [24] D.T. Favis-Mortlock, J. Boardman, A.J. Parsons, and B. Lascelles. Emergence and erosion: a model for rill initiation and development. *Hydrological Processes*, 14(11-12):2173–2205, 2000.
- [25] F.R. Fiedler and J.A. Ramirez. A numerical method for simulating discontinuous shallow flow over an infiltrating surface. *International Journal for Numerical Methods in Fluids*, 32(2):219–239, 2000.
- [26] G.R. Foster and L.D. Meyer. Mathematical simulation of upland erosion by fundamental erosion mechanics. *Present and Prospective Technology for Predicting Sediment Yields and Sources Agr. Res. Service Rep. ARS-S-40*, pages 190–207, 1975.
- [27] T. Gallouët, J.M. Hérard, and N. Seguin. Some recent finite volume schemes to compute euler equations using real gas eos. *International Journal for Numerical Methods in Fluids*, 39(12):1073–1138, 2002.

- [28] J.F. Gerbeau and B. Perthame. Derivation of viscous saint-venant system for laminar shallow water; numerical validation. *Discrete And Continuous Dynamical Systems-Series B*, 1, 2001.
- [29] N. Goutal and F. Maurel. Proceedings of the 2nd workshop on dam-break wave simulation. Technical report, Groupe Hydraulique Fluviale, Département Laboratoire National d'Hydraulique, Electricité de France, 1997.
- [30] W.H. Green and G. Ampt. Studies on soil physics: 1, flow of air and water through soils. *Journal of Agricultural Science*, 4:1–24, 1911.
- [31] J.M. Greenberg and A.Y. Leroux. A well-balanced scheme for the numerical processing of source terms in hyperbolic equations. *SIAM J. Numer. Anal.*, 33(1):1–16, 1996.
- [32] A. Harten. High resolution schemes for hyperbolic conservation laws. *Journal of Computational Physics*, 135(2):260–278, 1997.
- [33] A. Harten, P.D. Lax, and B. van Leer. On upstream differencing and godunov-type schemes for hyperbolic conservation laws. *SIAM Review*, 25, 1983.
- [34] J.M. Hervouet. *Hydrodynamics of free surface flows, modelling with the finite element method.*, volume ISBN 978-0-470-03558. Editions Wiley & Sons, 2007.
- [35] S. Jin. A steady-state capturing method for hyperbolic systems with geometrical source terms. *Mathematical Modelling and Numerical Analysis*, 35, 2001.
- [36] D. Jinkang, X. Shunping, X. Youpeng, C. Xu, and V.P. Singh. Development and testing of a simple physically-based distributed rainfall-runoff model for storm runoff simulation in humid forested basins. *Journal of Hydrology*, 336:334–346, 2007.
- [37] Randall J. Leveque. Balancing source terms and flux gradients in high-resolution godunov methods: The quasi-steady wave-propagation algorithm. *J. Comput. Phys*, 146:346–365, 1998.
- [38] Q.Q. Liu, L. Chen, J.C. Li, and V.P. Singh. Two-dimensional kinematic wave model of overland-flow. *Journal of Hydrology*, 291(1-2):28–41, 2004.
- [39] R.W. MacCormack. The effect of viscosity in hypervelocity impact cratering. *AIAA Paper*, pages 69–354, 1969.
- [40] I. MacDonald, M.J. Baines, N.K. Nichols, and P.G. Samuels. Steady open channel test problems with analytic solutions. Technical report 3, Department of Mathematics-University of Reading, 1995.
- [41] I. MacDonald, M.J. Baines, N.K. Nichols, and P.G. Samuels. Analytic benchmark solutions for open-channel flows. *Journal of Hydraulic Engineering-asce*, 123, 1997.

- [42] F. Marche. *Theoretical and Numerical Study of Shallow Water Models. Applications to Nearshore Hydrodynamics*. PhD thesis, Université de Bordeaux, France, 2005.
- [43] F. Marche. Derivation of a new two-dimensional viscous shallow water model with varying topography, bottom friction and capillary effects. *European Journal of Mechanics - B/Fluids*, 26(1):49 – 63, 2007.
- [44] R.G. Mein and C.L. Larson. Modeling infiltration during a steady rain. *Water Resources Research*, 9(2):384–394, 1973.
- [45] R.P.C. Morgan, J.N. Quinton, R.F. Smith, G. Govers, J.W.A. Poesen, K. Auerswald, G. Chisci, D. Torri, and M.E. Styczen. The european soil erosion model (eurosem): A dynamic approach for predicting sediment transport from fields and small catchments. *Earth Surface Processes and Landforms*, 23:527–544, 1998.
- [46] R. Moussa and C. Bocquillon. Approximation zones of the saint-venant equations for flood routing with overbank flow. *Hydrology and Earth System Sciences*, 4, 2000.
- [47] R. Najafi. Watershed modeling of rainfall excess transformation into runoff. *Journal of Hydrology*, 270(3-4):73–281, 2003.
- [48] M.A. Nearing, G.R. Foster, L.J. Lane, and S.C. Finkner. A process-based soil erosion model for usda water erosion prediction project technology. *Transactions of the ASAE*, 32:1587–1593, 1989.
- [49] D.K. Nguyen, Y.E. Shi, S. Wang, and T.H. Nguyen. 2d shallow-water model using unstructured finite-volumes methods. *Journal of Hydraulic Engineering*, 132(3):258–269, 2006.
- [50] G. Nord and M. Esteves. PSEM_2D: A physically based model of erosion processes at the plot scale. *Water Resources Research*, 41, 2005.
- [51] B. Perthame and C. Simeoni. A kinetic scheme for the saint-venant system with a source term. *Calcolo*, 38, 2001.
- [52] J.R. Philip. The theory of infiltration: 4. sorptivity and algebraic infiltration equations. *Soil Science*, 84, 1957.
- [53] L.A. Richards. Capillarity conduction of liquids through porous mediums. *Physics*, 1, 1931.
- [54] M. Rousseau. Modélisation des écoulements à surface libre : étude du ruissellement des eaux de pluie. Master’s thesis, Université de Nantes, available from: <http://dumas.ccsd.cnrs.fr/dumas-00494243/fr/>, september 2008.
- [55] M. Rousseau, O. Cerdan, A. Ern, O. Le Maître, and P. Sochala. Study of overland flow with uncertain infiltration using stochastic tools. *Advances in Water Resources*, 38(0):1–12, 2012.
- [56] V.P. Singh. Kinematic wave modelling in water resources: a historical perspective. *Hydrological Processes*, 15(4):671–706, 2001.

- [57] V.P. Singh. Is hydrology kinematic? *Hydrological Processes*, 16(3):667–716, 2002.
- [58] P. Sochala, A. Ern, and S. Piperno. Mass conservative bdf-discontinuous galerkin/explicit finite volume schemes for coupling subsurface and overland flows. *Computer Methods in Applied Mechanics and Engineering*, 198(27-29):2122–2136, 2009.
- [59] V. Souchère, O. Cerdan, N. Dubreuil, Y. Le Bissonnais, and C. King. Modelling the impact of agri-environmental scenarios on overland flow in a cultivated catchment (normandy, france). *Catena*, 61(3-4):229–240, 2005.
- [60] L. Tatard, O. Planchon, J. Wainwright, G. Nord, D. Favis-Mortlock, N. Silveira, O. Ribolzi, M. Esteves, and C. Huang. Measurement and modelling of high-resolution flow-velocity data under simulated rainfall on a low-slope sandy soil. *Journal of Hydrology*, 48(1-2):1–12, 2008.
- [61] W.C. Thacker. Some exact solutions to the non-linear shallow-water wave equations. *Journal of Fluid Mechanics*, 107, 1981.
- [62] P.L. Viollet, J.P. Chabard, P. Esposito, and D. Laurence. *Mécanique des fluides appliquée, écoulements incompressibles dans les circuits, canaux et rivières autour de structures et dans l’environnement*. Presses de l’Ecole Nationale des Ponts et Chaussées, 2002.
- [63] J. Wainwright, A.J. Parsons, E.N. Müller, R.E. Brazier, D.M. Powell, and B. Fenti. A transport-distance approach to scaling erosion rates: 3. evaluating scaling characteristics of mahleran. *Earth Surface Processes and Landforms*, 33(7):1113–1128, 2008.
- [64] S. Weill, E. Mouche, and J. Patin. A generalized richards equation for surface/subsurface flow modelling. *Journal of Hydrology*, 366(1–4):9–20, 2009.
- [65] D.A. Woolhiser, R.E. Smith, and D.C. Goodrich. Kineros, a kinematic runoff and erosion model: Documentation and user manual. 1990.